

2012

A Silica Single-Mode Fibre-Chalcogenide Multimode Fibre-Silica Single-Mode Fibre Structure

Pengfei Wang

Technological University Dublin, pengfei.wang@tudublin.ie

Ming Ding

University of Southampton

Lin Bo

Technological University Dublin

See next page for additional authors

Follow this and additional works at: <https://arrow.tudublin.ie/engscheceart>



Part of the [Electrical and Electronics Commons](#)

Recommended Citation

Wang, P., Ding, M., Bo, L., Semenova, Y., Wu, Q. and Gerald Farrell: A Silica Single-Mode Fibre-Chalcogenide Multimode Fibre-Silica Single-Mode Fibre Structure. *Photonics Letters of Poland*, Vol.4, issue 4, 2012, pp.143-145. DOI: 10.4302/plp.2012.4.08

This Article is brought to you for free and open access by the School of Electrical and Electronic Engineering at ARROW@TU Dublin. It has been accepted for inclusion in Articles by an authorized administrator of ARROW@TU Dublin. For more information, please contact arrow.admin@tudublin.ie, aisling.coyne@tudublin.ie.



This work is licensed under a [Creative Commons Attribution-NonCommercial-Share Alike 4.0 License](#)

Authors

Pengfei Wang, Ming Ding, Lin Bo, Yuliya Semenova, Qiang wu, and Gerald Farrell

A silica single-mode fibre-chalcogenide multimode fibre-silica single-mode fibre structure

Pengfei Wang^{1,2*}, Ming Ding², Lin Bo¹, Yuliya Semenova¹, Qiang Wu¹, and Gerald Farrell¹

¹Photonics Research Centre, Dublin Institute of Technology, Kevin Street, Dublin 8, Ireland

²Optoelectronics Research Centre, University of Southampton, Southampton SO17 1BJ, United Kingdom

Received December 05, 2012; accepted December 30, 2012; published December 31, 2012

Abstract—In this letter we theoretically and experimentally investigate a single-mode-multimode-single-mode (SMS) structure based on chalcogenide (As₂S₃) multimode fibre and silica single-mode fibres. The experimental results show a general agreement with the numerical simulation results based on a wide angle-beam propagation method (WA-BPM). Multimode interference variation was observed as a result of photo-induced refractive index changes arising from either localized laser irradiation at a wavelength of 405 nm or the use of a UV lamp. Our result provides a platform for the development of compact, high-optical-quality, and robust photonic nonlinear devices.

Recently multimode interference (MMI) occurring in a single-mode–multimode–single-mode (SMS) fibre structure has been studied for applications in novel optical devices, e.g. displacement sensor [1], stain and temperature sensor [2], refractometer sensor [3] and edge filter for wavelength measurements [4]. These optical devices, based on such an SMS fibre structure, offer all-fibre solutions for optical communications and sensing with the advantages being the ease of packaging and connection to other optical fibre systems.

Chalcogenides are rapidly establishing themselves as technologically superior materials for emerging applications in non-volatile memory and high speed switching [5] and have been considered for a range of other optoelectronic technologies. Chalcogenide glasses offer a wealth of attractive properties such as exceptionally high nonlinearity, photosensitivity, ultrafast nonlinear response, low phonon energy matrix, ability to be doped with active elements including lanthanides and transitional metals, and the possibility to form detectors, lasers and amplifiers. Unlike any other optical material, they have been formed into a multitude of shapes, including optical fibres, thin films, bulk optical components, microsphere resonators, metamaterials and nanoparticles, patterned by CMOS compatible processing at the sub-micron scale. To date, applications including ultrafast all-optical switching, supercontinuum generation, broadband wavelength conversion, all-optical signal processing, ultrafast pulse characterization and Raman fibre lasers have been demonstrated extensively using chalcogenide glass fibres [6-8].

* E-mail: pengfei.wang@dit.ie

In this letter we present an investigation of light propagation within an SMS fibre structure based on chalcogenide and silica fibres. A chalcogenide fibre based multimode interference device is fabricated and packaged by using UV curing. Due to the photo-induced refractive index changes in the chalcogenide glass material, the spectral response achieved for multimode interference also varies with both power and irradiation position for a localized laser irradiation with a maximum output power of 10mW at a wavelength of 405nm. The peak shift of the spectral responses of 2nm has been realized and we also achieved a power variation at 1565.4nm as high as 8.94dB depending on different localized laser irradiation positions along the chalcogenide fibre. The fabricated device offers the potential for low-cost, robustly assembled fully integrated all-optical switching and tunable filter devices due to its unique high nonlinearity and ease of fabrication.

An SMS fibre structure consists of input and output silica single-mode fibres (SMFs) with a short section of multimode fibre (MMF) sandwiched between them as shown in Fig. 1. A chalcogenide multimode fibre section is sandwiched between two standard silica single-mode fibres and forms a typical fibre multimode interferometer.

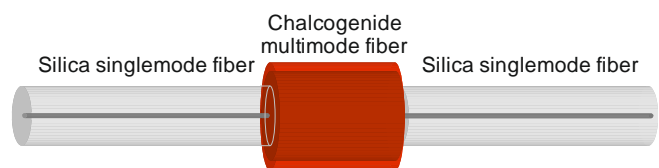


Fig. 1. Schematic of an SMS fibre structure based on silica single-mode fibre-chalcogenide multimode fibre-silica single-mode fibre.

The SMS spectral properties were simulated using a WA-BPM presented in [9]: as light propagates in the MMF section, the modal interference field at a propagation distance z from the input can be given by:

$$E(r, z) = \sum_{m=1}^M \varphi_m \psi_m(r) \exp(i\beta_m z) \quad (1)$$

where φ_m is the excitation coefficient of each eigenmode [which can be expressed by the overlap integral between the optical distribution field of input SMF $E(r, 0)$ and

$\psi_m(r)$], $\psi_m(r)$ is the field profile of LP_{0m} and β_m is the propagation constant of each eigenmode propagating within the multimode fibre. The modal interference generated in the MMF section is shown in Fig. 2 (a), presenting the amplitude distributions field of the propagating optical fields, as it evolves along the length of the MMF section. To calculate the coupling loss of the optical field $E(r,z)$ at a propagation distance z from the output SMF, the overlap integration between the light field $E(r,z)$ and the eigenmode of the output SMF can be used:

$$L_s(z) = 10 \log_{10} \left(\frac{\left| \int_0^\infty E(r,z) F(r) r dr \right|^2}{\int_0^\infty |E(r,z)|^2 r dr \int_0^\infty |F(r)|^2 r dr} \right) \quad (2)$$

where $F(r)$ is the fundamental mode of the output SMF. It is assumed the output SMF has the same fibre parameters as the input SMF, therefore $F(r) = E(r,0)$. Figure 2(b) presents the coupling loss to the output SMF as a function of propagation distance of the MMF field. Both Fig. 2(a) and (b) show that the first significant multimode interference occurs for $z > 10$ mm.

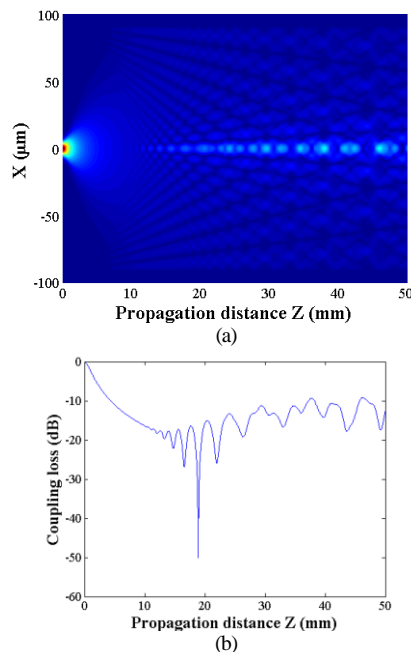


Fig. 2. (a) Light propagation within the chalcogenide multimode fibre; (b) Calculated coupling loss to output single-mode fibre for different chalcogenide multimode fibre lengths when the wavelength of the input light is 1550 nm.

In Fig. 2(b), it can be seen that the coupling loss reaches a maximum value of -50 dB at a propagation position of $z = 18.91$ mm. Compared with the previously calculated results shown in [9], the calculated results here show that the eigenmode interference within the MMF section is

determined by both the size and the refractive index of the MMF core. The chalcogenide fibre used in the experiments is a commercial step-index multimode fibre provided by Oxford Electronics, with an As_2S_3 core (OD=180 μ m) and As_xS_{1-x} cladding of lower refractive index (OD=275 μ m). The chalcogenide multimode fibre cross section is shown in Fig 3.

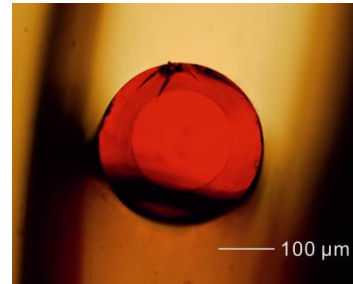


Fig. 3. Microscope image of chalcogenide multimode fibre cross section.

The SMS sample was fabricated by sandwiching the commercial chalcogenide multimode fibre between two silica SMFs. The fibre cores were aligned using 3D translation stages, and the alignment was maintained by embedding the fibre joints into a UV curable polymer with a low refractive index. Figure 4 shows the experimental setup for fabricating the SMS fibre structure. The transmission spectra of the fabricated hybrid SMS fibre device were then recorded using an amplified spontaneous emission (ASE) light source (1520~1570 nm) and an optical spectrum analyzer (OSA YOKOGAWA AQ6370).

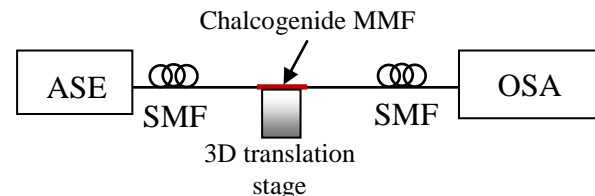


Fig. 4. Schematic of experimental setup.

Figure 5(a) presents the calculated and measured transmission spectra of the hybrid SMS structure. The results show a general agreement with theoretical predictions. The discrepancy between the calculated and measured results could be due to slight misalignment between SMFs and MMF. The effect of the manufacturing tolerances on the core diameters of the MMF and SMFs and the approximations made in the calculations (simulated transmission for an SMS includes some approximations, such as the Padé (3, 3) approximate operator). In order to demonstrate the stability of the fabricated SMS, Fig. 5(b) presents the transmission spectra of the SMS fibre device as they vary with time before/after the UV glue curing. The changes in the

transmission spectra are due to the temperature change and further curing of the polymer glue.

It is well known that chalcogenide glasses have high photosensitivity, namely the refractive index can vary with external laser irradiation. Therefore the spectral response achieved from the multimode interference within the SMS device based on a chalcogenide MMF can also be tuned by laser irradiation. In order to demonstrate this effect, the chalcogenide MMF part in the SMS fibre structure was irradiated and scanned by a localized CW laser with a maximum output power of 10mW at $\lambda=405$ nm. The laser spot size on the chalcogenide MMF was estimated to be circa $7 \times 10^{-4} \text{cm}^2$, providing an irradiation intensity of $1.43 \times 10^4 \text{mW/cm}^2$. The resulting changes in the transmission spectrum were monitored by the OSA in real time.

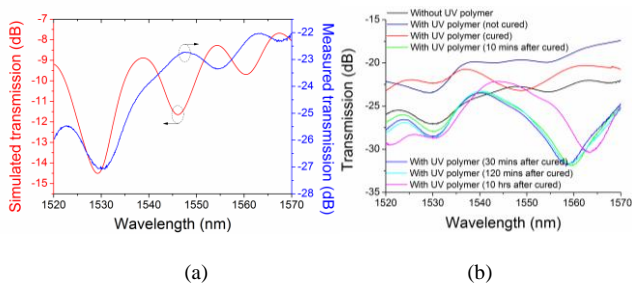


Fig. 5. (a) Calculated and measured spectral responses of the hybrid SMS device over a wavelength range of 1520~1570nm; (b) change in the SMS transmission spectra before/after UV glue curing.

Figure 6 shows that the spectral response red-shifts by 2 nm and power variations as high as 8.94 dB at $\lambda=1565.4$ nm were observed when the localized laser irradiated at the position of $z \sim 5.5$ mm along the chalcogenide fibre. The entire chalcogenide MMF was then irradiated by a broadband UV lamp (Hamamatsu L9588-02A, wavelength range: 240-400nm) with an average output power of 410mW/cm^2 . Figure 6 shows that significant changes of the SMS spectrum occur and the power variation at 1563.3nm as high as 7.57dB can be achieved.

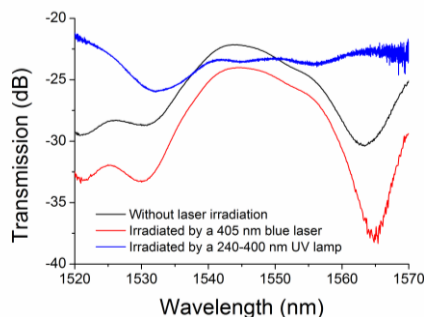


Fig. 6. Transmission spectra of the chalcogenide SMS device as fabricated, after irradiation by a 405nm laser and after exposure to a broadband UV lamp.

In conclusion, as a first proof of concept, we have proposed and demonstrated a chalcogenide MMF based SMS structure. The experimental characterization showed a general agreement with numerical simulations. Due to the high photosensitivity of the chalcogenide glass material itself, the chalcogenide SMS fibre structure can be utilized to form a range of functionalities over near- and mid-IR wavelength ranges, such as a tunable filter and an all-optical switching fibre device. This geometry may become a promising platform for linear signal processing devices with thresholds orders of magnitudes lower than conventional silica based fibre devices.

P. Wang is funded by the Irish Research Council, co-funded by the EU Marie-Curie Actions under FP7. Q. Wu gratefully acknowledges the support of Science Foundation Ireland under grant no. 07/SK/I1200.

References

- [1] Q. Wu, Y. Semenova, P. Wang, A.M. Hatta and G. Farrell, *Meas. Sci. Technol.* **22**, 025203 (2011).
- [2] S.M. Tripathi, A. Kumar, R.K. Varshney, Y.B.P. Kumar, E. Marin, J.-P. Meunier, *J. Lightwave Tech.* **27**, 2348 (2009).
- [3] P. Wang, G. Brambilla, M. Ding, Y. Semenova, Q. Wu, G. Farrell, *Opt. Lett.* **36**, 2233 (2011).
- [4] Q. Wang, G. Farrell, *Micro. Opt. Tech. Lett.* **48**, 900 (2006).
- [5] C. Grillet, S.N. Bian, E.C. Magi, B.J. Eggleton, *Appl. Phys. Lett.* **92**, 171109 (2008).
- [6] M. Asobe, H. Kobayashi, H. Itoh, T. Kanamori, *Opt. Lett.* **18**, 1056 (1993).
- [7] S. Shakeri and M. Hatami, *J. Opt. Soc. Am. B* **27**, 679 (2010).
- [8] B.J. Eggleton, B. Luther-Davies, K. Richardson, *Nature Photonics* **5**, 141 (2011).
- [9] P. Wang, G. Brambilla, M. Ding, Y. Semenova, Q. Wu, G. Farrell, *J. Opt. Soc. Am. B* **28**, 1180 (2011).